Preparation of Spherical Nanocomposites Consisting of Silica Core and Polyacrylate Shell by Emulsion Polymerization

Tsutomu Mizutani,[1] Koji Arai,[1] Masatoshi Miyamoto,[2] Yoshiharu Kimura[3]

[1]*R&D Center, Mizutani Paint Mfg, Co. Ltd., 3–9, Nishi-mikuni-4-chome, Yodogawa-ku, Osaka, 532-0006, Japan*
[2]*Center for Bio-Resource Field Science, Kyoto Institute of Technology, Matsugasaki, Sakyo, Kyoto 606-8585, Japan*
[3]*Department of Polymer Science, Kyoto Institute of Technology, Matsugasaki, Sakyo, Kyoto 606-8585, Japan*

Received 21 July 2003; accepted 4 March 2005
DOI 10.1002/app.22503
Published online in Wiley InterScience (www.interscience.wiley.com).

ABSTRACT: Nanocomposite particles consisting of silica (inorganic core) and polyacrylate (organic shell) were prepared in a form of emulsion by a new and simple method—the emulsion polymerization of acrylic monomers in the presence of silica sol. The key technique of the present emulsion polymerization, which made the formation of the nanocomposites successful, is the usage of nonionic surfactant above its cloud point. The morphology of the composite was investigated by DLS, AFM, and TEM, which clearly showed formation of the core-shell-type particles. A transparent film was prepared by casting the emulsion, which showed high resistibility against organic solvents. © 2005 Wiley Periodicals, Inc. J Appl Polym Sci 99: 659–669, 2006

Key words: core-shell polymers; emulsion polymerization; nanocomposites; silicas

INTRODUCTION

Nanocomposites comprised of organic polymers and inorganic nano-particles are nowadays widely used for various industrial purposes, for example, coatings, adhesives, rubber reinforcements, and biomedical and electronic industrial materials.[1–3] In these composites, inorganic nano-particles improve the physical properties of the base polymers or add proper functions to them. Although various inorganic materials are available in a form of nano-particles, silica is famous in its chemical stability, high surface area, and easy availability. Therefore, nanocomposites containing silica, especially silica gel, have attracted a great deal of attention.

The properties of nanocomposites are greatly influenced by the dispersing degree of inorganic components in the base polymers. Although nanocomposites have been reported to be prepared by simple blending via high shear stirring or ball milling, the dispersing degree of inorganic nano-particles was obviously insufficient.[4] So, many approaches have been done to bestow on the inorganic component, affinity toward the base polymer.[5] Silica nano-particles are often treated with silane coupling agents for this purpose, although such treatment is still insufficient in many cases.[6] Encapsulation of inorganic particles with a polymer is another, more effective approach to improve its affinity to the base polymer.[5,7–16]

Common approaches of encapsulating inorganic particles are: (1) treatment with the polymer synthesized in advance, and (2) polymerization on the particle surface. The former has the advantages of simplicity and high efficiency. The latter's advantages are that the polymerization and the encapsulation can be done simultaneously and the introduction of functional groups into the encapsulating polymers is possible. To capsulate the particles by polymerization, both initiator and monomer have to gather around the particle surface. However, a nano-scale silica particle, silica sol, has negative charges due to SiO^- and silanol-type hydroxyl groups on its surface, which makes the particle surface highly lipophobic. Nakamae et al. have examined the polymerization started from azo groups introduced on the silica surface by the chemical modification of the silanol group.[17] In another approach, a radical initiator having a cationic charge was employed for the polymerization, which was absorbed and started the polymerization on the particle surface.[18]

Efficient capsulation has also been conducted by the proper choice of monomer. Armes and coworkers have developed the surfactant-free synthesis of vinyl polymer/silica nanocomposite particles by copolymerizing 4-vinylpyridine in the presence of silica sol.[19–21] Concerning the surfactant, the use of ionic-

Correspondence to: M. Miyamoto (miyamoto@ipc.kit.ac.jp).
Contract grant sponsor: Japan Science and Technology Agency.

surfactant having opposite electronic charge to the particle has previously been reported; the absorbed surfactant on the particle surface is considered to improve the affinity to the organic monomer.[22,23]

In the present article, we postulate a new method to prepare nanocomposites by encapsulation. Our method is distinguished from the other methods by the ease of the procedure and the high effectiveness in preparing core-shell type nano-particles. Namely, nanocomposites consisting of silica nano-particles as the core and polyacrylate shell were prepared by the simple emulsion polymerization of acrylates using nonionic surfactant in the presence of silica sol. No special monomer having a high affinity to silica, such as 4-vinylpyridine, is required in the present study; monomers for this work were *n*-butyl acrylate and methyl methacrylate, although the monomer mixture contained a small amount of methacrylic acid to improve the stability of the resulting emulsion. The key point of this approach is to use the nonionic surfactant above its cloud point in the polymerization to induce the deposition of the surfactant onto the silica sol interface, which enhances the affinity of the silica surface to the organic materials. The formation of nanocomposite was confirmed, and its solubility against several solvents was also investigated.

EXPERIMENTAL

Materials

The colloidal silica, silica sol, used in the present study was ADELITE AT-50, whose diameter was reportedly 20 ~ 30nm. It was sold by Asahidenka Co. as a 50 wt % aqueous dispersion. ADECA REASOAP NE-10 and NE-30 are poly(ethylene oxide)-type reactive nonionic surfactants are shown in Structure 1.

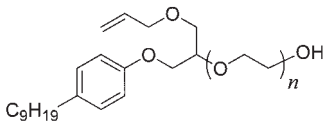

NE-10; n=10

NE-30; n=30

Structure 1

They were also purchased from Asahidenka Co. Sodium dodecylbenzenesulfonate used in this study was sold by Kao Co. under the trade name of NEOPELEX F-25. Methyl methacrylate (MMA), *n*-butyl acrylate (*n*-BA), methacrylic acid (MAA), and other chemicals were industrial grade reagents and were used as received.

Polymerization procedure

A typical procedure is as follows. Prior to the polymerization, a monomer mixture was prepared, which consisted of MMA (69 g), *n*-BA (130 g), and MAA (1.0 g). Into a 1 L flask equipped with a condenser, a dropping funnel, and a mechanical stirrer was charged 340 g of AT-50 under nitrogen. A solution of 0.5 g of ammonium peroxydisulfate (APS) and 5.0 g of NE-10 in 140 g of water was added dropwise to AT-50 with vigorous stirring at 60°C. After the addition, the temperature of the mixture was raised to 70°C. To the mixture was added dropwise 5 g of the monomer mixture, and the contents were kept at 70°C for 1h. Then, a mixture of 0.6 g of APS and 24 g of F-25 in 50 g of water and the rest of the monomer mixture were added dropwise sequentially. The reaction mixture was kept at 70°C for an additional hour to complete the polymerization. After the solution was cooled to room temperature, 3.6 g of an aqueous ammonia solution (25 wt %) was added to the resulting emulsion to control its pH in a proper range.[9,10]

The emulsion polymerization initiated by a redox system was carried out in an analogous procedure, in which 0.8 g of sodium hydrogen sulfite was added into the monomer mixture described above and the whole reactions were carried out at 50°C instead of 70°C.

Instrumentation

Dynamic force mode atomic force micrograms were measured on a Shimadzu SPM-9500J3 microscope. The sample was prepared by diluting the emulsion 200 times with distilled water, casting on a mica plate, and drying at room temperature for one week. Energy filtering transmission electron microscopic analysis was performed on a LEO 912 Carl Zeiss EFTEM with in-column ω filter at 120 kV of acceleration voltage. Transmission electron micrograms were taken on a Hitachi H7100 at 125kV of acceleration voltage. The measurements of particle size and size distribution were performed on an Otsuka Electronics electrophoretic light scattering spectrophotometer ELS-8000 (light source: He-Ne laser). The sample was diluted 3000 times with distilled water before the measurements.

Preparation of nanocomposite film

A sample film was prepared by casting the emulsion on a polyethylene sheet with an applicator (0.2 mm). The film was dried at 50°C for 16 h or at room temperature for one week.

Solubility of the film to organic solvents

The sample films (5 × 5 × 0.2 mm, 50mg) were immersed in 6.0 g of the solvent and kept at 50°C for 24 h.

TABLE I
Preparation of Nanocomposite Emulsions by Emulsion Polymerization

						Product					
							Appearance[a]		Averaged diameter (nm)		
Run no.	Nonionic surfactant	Feed ratio Silica/Monomer (wt/wt)	Initiator	Temp. (°C)	Yield (%)	Abbrev.	Just after preparation	After 1 day	Marquadt method	Cumulant method	Poly-dispersity[b]
1	NE-10	85/100	APS	70	100	NCE(46)	h.e.	h.e.	111 ± 54	92	0.21
2	NE-10	85/100	redox	50	100	—	p.a.e.	gel	—	—	—
3	NE-30	85/100	APS	70	100	—	p.a.e.	gel	98 ± 15, 630 ± 200	479	0.24
4	NE-30	85/100	redox	50	100	—	p.a.e.	gel	—	—	—
5	none	85/100	APS	70	98	—	h.e.	h.e.	35 ± 6, 158 ± 46	117	0.20
6	NE-10	0/100	APS	70	99	OE(0)	h.e.	h.e.	101 ± 21	97	0.0031
7	NE-10	43/100	APS	70	100	NCE(30)	h.e.	h.e.	113 ± 46	107	0.21
8	NE-10	200/100	APS	70	99	NCE(67)	h.e.	h.e.	97 ± 55	85	0.25

[a] h.e., homogeneous emulsions; p.a.e., partly aggregated emulsion.
[b] Determined by the Cumulant method.

The solubility of the film was roughly judged from the appearance of the remaining film in the solvent. For determining the solubility to DMF, 250 mg of the sample film was immersed in 30 g of DMF at 50°C for 24 h. The insoluble portion was separated by centrifugation (at 10,000 rpm, for 15 min.) and washed with 30 g of ethyl acetate. After the above centrifugation-washing procedure was repeated 3 times, the film was dried under vacuum and weighed.

RESULTS AND DISCUSSION

Synthesis of nanocomposite emulsion

The ultra fine colloidal silica used in the present study was in a form of 50 wt % aqueous dispersion, whose pH was set to around 10 to stabilize it. Therefore, the surface of the silica particle, whose diameter was reported to be 20 ~ 30 nm, was highly hydrophilic because of the partial ionization of terminal hydroxysilyl groups to silicate anions. To cover such a hydrophilic silica particle with an organic layer effectively, we planned to develop a new method to conduct the radical polymerization of acrylates on its very surface. After many failures, we developed a novel procedure of emulsion polymerization with the simultaneous usage of nonionic and anionic surfactants. The key features of our method are to use a nonionic surfactant having a relatively low cloud point and to carry out the emulsion polymerization at a higher temperature than the cloud point. Consequently, the results of the emulsion polymerization to produce nanocomposite particles were greatly influenced by the selection of nonionic surfactant (Table I). A mixture of acrylic monomers consisting of butyl acrylates (65%), methyl methacrylate (34.5%), and acrylic acid (0.5%) was adopted for the emulsion polymerization to adjust T_g of the resulting organic shell to a desired temperature; T_g of the above composition is calculated as −23°C.

The following optimized protocol to prepare the nanocomposite emulsion was developed after a large number of careful experiments with changing surfactant, temperature, feed ratio, and other polymerization conditions and the procedures. The process to optimize the protocol was so complicated that we do not intend to indicate it here. Instead, we indicate the optimized protocol first and verify its appropriateness later.

The optimized protocol is complicated in comparison with the conventional emulsion polymerization, and it consists of four steps: surface modification, prepolymerization, dissolution, and postpolymerization. All steps were indispensable to prepare the stable emulsion of nanocomposite. As it is difficult to understand the role of each step, we illustrate the supposed states of the silica particles schematically in relation to the individual operations in Figure 1. A more detailed protocol is shown in the Experimental section.

Optimized protocol

Surface modification step. First, the colloidal silica was mixed with NE-10 at 60°C. NE-10 is a nonionic surfactant having an allyl group and an oligo(oxyethylene) chain (DP = 10), and its cloud point is reportedly 40°C. According to the addition of NE-10, the turbidity of the mixture slightly increased, but no drastic change in appearance was observed. At this stage, a large part of the surfactant molecules are considered to be absorbed onto the silica particles as the poly(oxyethylene) block in the surfactant can bond with the hydroxysilyl groups through hydrogen bondings,

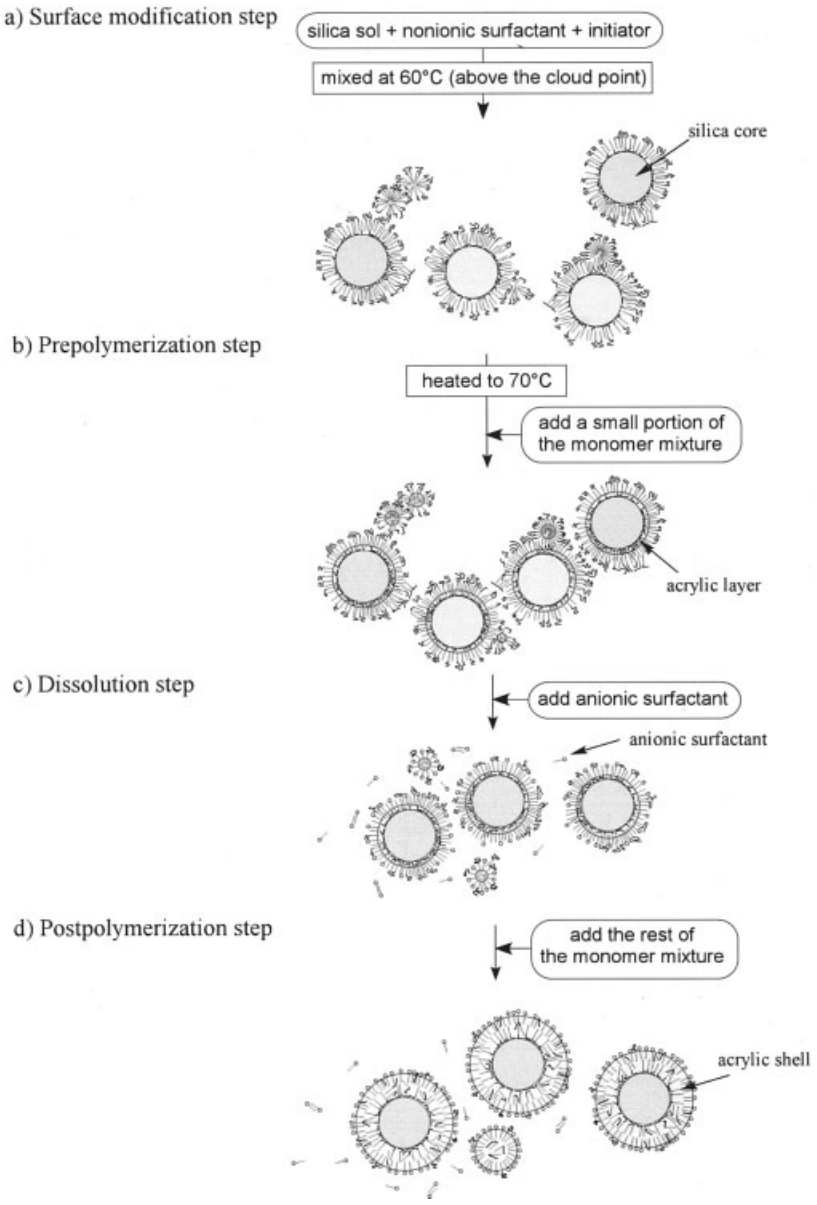

Figure 1 Schematic illustration for the four-step optimized protocol to prepare the nanocomposite emulsion: (a) Surface modification step, (b) Prepolymerization step, (c) Dissolution step, and (d) Postpolymerization step.

while its affinity to water is almost lost as the temperature is higher than the cloud point of NE-10 [Fig. 1(a)]. The resulting surfactant layer formed on the surface gives a hydrophobic property to the silica particle, which makes polymerization on the silica surface possible.

The surface modification of silica by the surfactant can induce coaggregation between the silica particles and the surfactant molecules to form large secondary particles due to the hydrophobic interaction between the organic parts of the surfactant molecules, which would increase the turbidity of the system. However, the small change in appearance as well as dynamic light scattering (DLS) measurement of the finally produced emulsion (*vide infra*) proved that the extent of coaggregation was essentially low.

Prepolymerization step. Then, the system was heated to 70°C, and a small portion of the monomer mixture, a quantity equal to that of the nonionic surfactant, was introduced into the suspension and the system was kept for 1 h with vigorous stirring at 70°C. No significant change in the appearance of the suspension was found during this step. Such prepolymerization is often adopted in the usual emulsion polymerization to uniformize the particle size. Actually, the polydispersity of the particle size prepared according to this protocol in the absence of the silica sol was found to be very narrow (*vide infra*).

In the presence of silica sol, a procedure lacking the prepolymerization step failed to prepare a stable emulsion. Therefore, the role of this step is presumed as follows. Although the nonionic surfactant has al-

most lost its surface activity at this temperature, the monomer liquid is suspected to penetrate slowly into the nonionic surfactant layer of the modified silica. As the radical initiator, APS, had already been added into the system, radical copolymerization among the monomers and the allyl group in the nonionic surfactant proceeded during this period, which fixed the nonionic surfactant shell covering the silica core [Fig. 1(b)].

Dissolution step. Then, the anionic surfactant, sodium dodecylbenzenesulfonate (SDS), was introduced to the turbid suspension. The turbidity of the system paled to same extent after the addition. The anionic surfactant molecules will array on the nanocomposites' surface to give them affinity to water; each of the nanocomposites now has a thin organic shell [Fig. 1(c)].

Postpolymerization step. Then, the rest of the monomer mixture was introduced into the system. The monomer liquid penetrates into the anionic surfactant layer covering the silica particle to form a droplet containing the modified silica core. An initiating radical jumps into the droplet and starts the polymerization, as in the usual case of emulsion polymerization, to produce organic (shell)-inorganic (core) hybrid nanoparticles [Fig. 1(d)].

The result of the polymerization according to the optimized protocol is indicated in run 1 of Table I. The polymerization proceeded almost quantitatively, and gave a stable emulsion containing nano-scale particles, whose average diameter was determined as 111 nm by DLS [Fig. 2(b)]. The emulsion was found to be very stable. Even after the emulsion stood for several months, no obvious change was observed.

Morphology of the nanocomposite

The DLS chart of the silica sol, AT-50, is shown in Figure 2(a). The average diameter of AT-50 was calculated as 52 ± 15 nm on the basis of scattering intensity by the Marquadt method. This value was revised to 35 ± 8 nm considering the fact that the scattering intensity is proportional to molecular mass, which increases as the cube of the diameter as far as the density of particles is constant. This assumption, however, cannot be applied to nanocomposite emulsions as the density of individual particles can vary from that of silica (2.2) to that of the organic component (1.0) depending on its silica content. Therefore, we adopted average diameters calculated by the Marquadt method without correction shown in Table I, which will give overestimated values. In the Table, the average diameters and polydispersity indices given by the Cumulant method are also shown, as reference.

The TEM image of AP-50 is shown in Figure 3(a). Although the particles aggregated with each other during the drying process of the sample for the TEM measurement, the average diameter of the primary silica particles was estimated as 30 ± 8 nm from Figure 3(a), which is in good agreement to that obtained from DLS after correction.

Figure 3(b) shows a TEM image of the nanocomposite particles prepared according to the optimized protocol, in which organic shells can be seen around the silica core as parts being light in color. Although the particles aggregated with each other during the drying process for the TEM analysis, it is obvious that almost all primary particles contained a silica core. Although a few organic particles free from the inorganic core are found in the Figure, it is noteworthy that no silica particle uncovered by the polymer shell is detected in the micrograph. As the emulsion polymerization proceeded almost quantitatively in any run in Table I, the inorganic content can be calculated from the feed ratio of AT-50 and the monomer mixture. Hereafter, the nanocomposite emulsion is abbreviated as NCE, attaching the inorganic content after drying (wt %) in parentheses, that is, NCE(46) for run 1 in Table I.

The average diameter of the nanocomposite particles was difficult to estimate from Figure 3(b) as the boundaries among the particles were obscure, although the diameter can be determined for isolated particles. For example, the particle located at the lower left in Figure 3(b), which is indicated by an arrow, has outside diameter of 58 nm and inside diameter of 39 nm. The theoretical ratio between the radii can be calculated from the feed ratio and the densities of the silica and organic parts as 0.65, which agrees well with the observed value ($39/58 = 0.67$).

The almost complete encapsulation of the silica core by the organic shell was proved by energy-filtering transmission electron microscopy (EFTEM), which makes it possible to observe elemental maps of energy filtered diffraction patterns. Figure 4(a) shows a usual TEM image of NCE(46). Figure 4(b) is the carbon elemental map revealing the acrylic shells, and Figure 4(c) is the silicon elemental map revealing the silica cores. From the comparison of these Figures, it is obvious that the organic part penetrates into the borderline between the silica cores and separates them. Thus, the large secondary particle was formed after the formation of the core-shell type nanocomposite particles during the drying process for TEM or during the postpolymerization step.

Figure 4 again shows that some organic particles, which did not contain silica cores, contaminated the nanocomposites. However, it is obvious that effectively every silica particle was covered by the organic shell.

The average diameter of the nanocomposite particles is estimated as 42 ± 9 nm from Figure 4. The DLS measurement of NCE(46) (Fig. 2b), on the other hand, gave the average diameter as 111 nm by the Marquadt

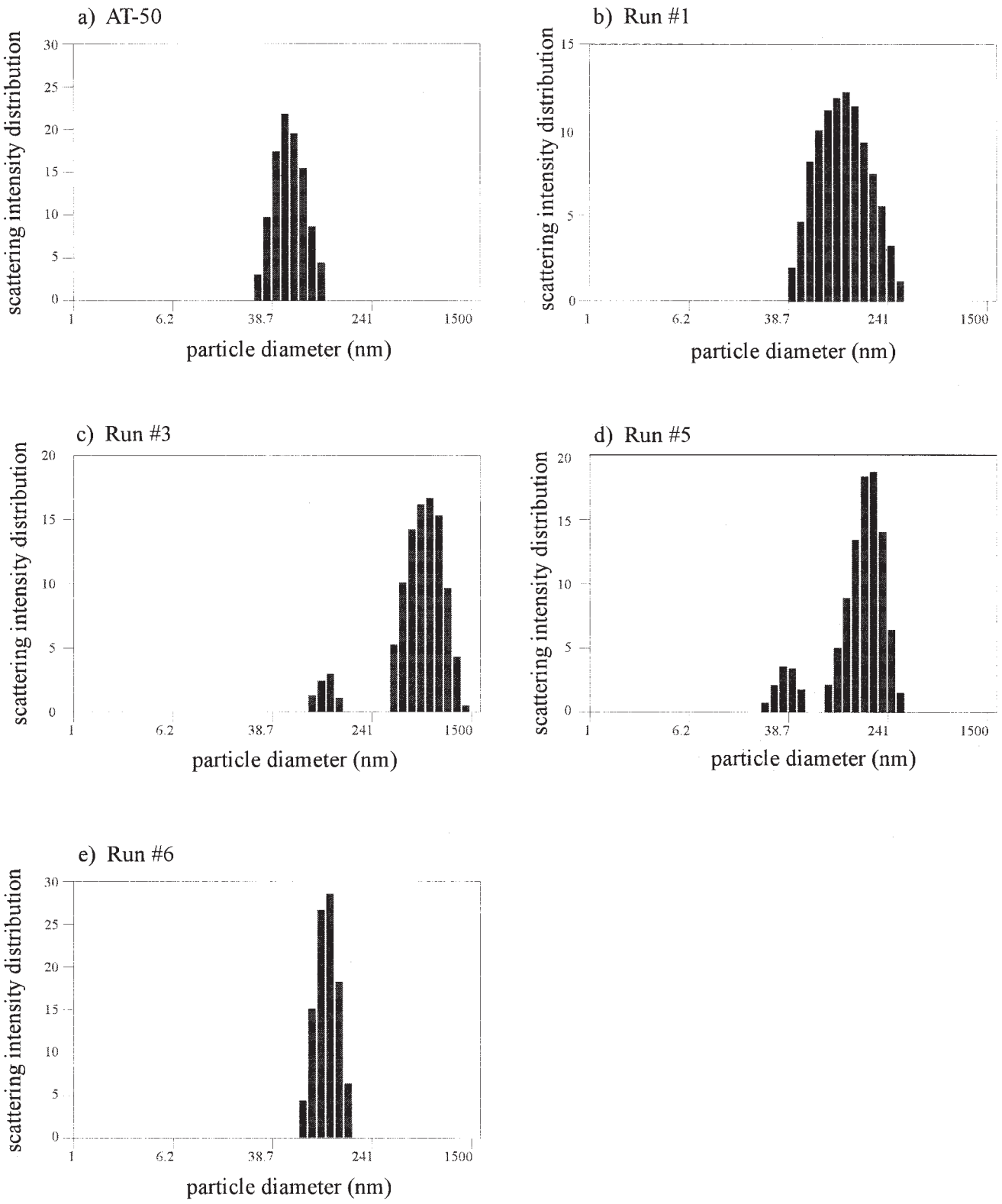

Figure 2 Size distributions of the nanoparticles measured by DLS: (a) AT-50, (b) Run #1, (c) Run #3, (d) Run #5, and (e) Run #6.

method, which was revised to 63 nm with the assumption that the density of the particles is constant. This value is considerably higher than that from EFTEM. A part of this difference is ascribed to the intrinsic difference in analytical method, as DLS gives hydrodynamic radius. This difference, however, will suggest

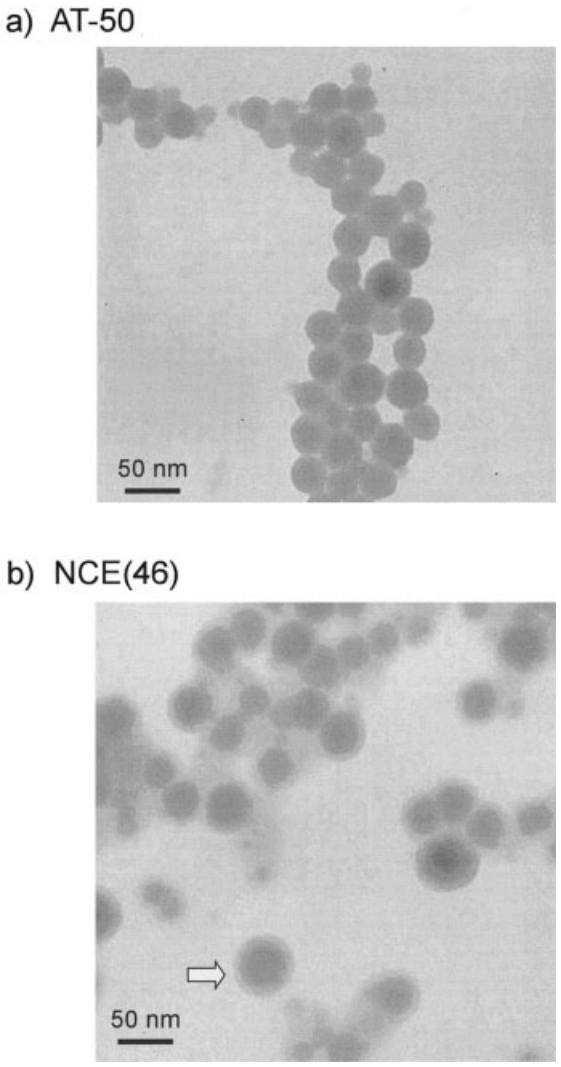

Figure 3 TEM images of: (a) AT-50 and (b) NCE(46).

that NCE contains multi-core particles to some extent, which are considered to be produced partly during the surface modification step and grew during the pre- and postpolymerization steps without suffering dissociation. The multi-core particles may also be produced by the aggregation of the primary nano-particles. The content of the multi-core particles in NCE(46) is, however, judged to be small from DLS.

Verification of the protocol

The results for experiments to verify the optimized protocol are shown in runs 2–6 in Table I. The emulsion polymerization in the absence of silica sol (run 6), which was carried out in an analogous multi-step protocol, gave an organic emulsion (OE(0)) having 101 nm of average diameter on the basis of scattering intensity [Fig. 2(e)], which is revised to 86 nm considering the molecular mass. The size distribution of OE(0) was very narrow, which is the result of the multi-step polymerization procedure containing the prepolymerization step. The size distribution of NCE(46) broader than that of OE(0) will be another evidence that it contains multi-core particles to some extent.

Even in the absence of nonionic surfactant (run 5), the polymerization of acrylic monomer proceeded quantitatively and an emulsion was obtained. However, DLS analysis of the sample indicated that the emulsion contained uncovered silica particles. Figure

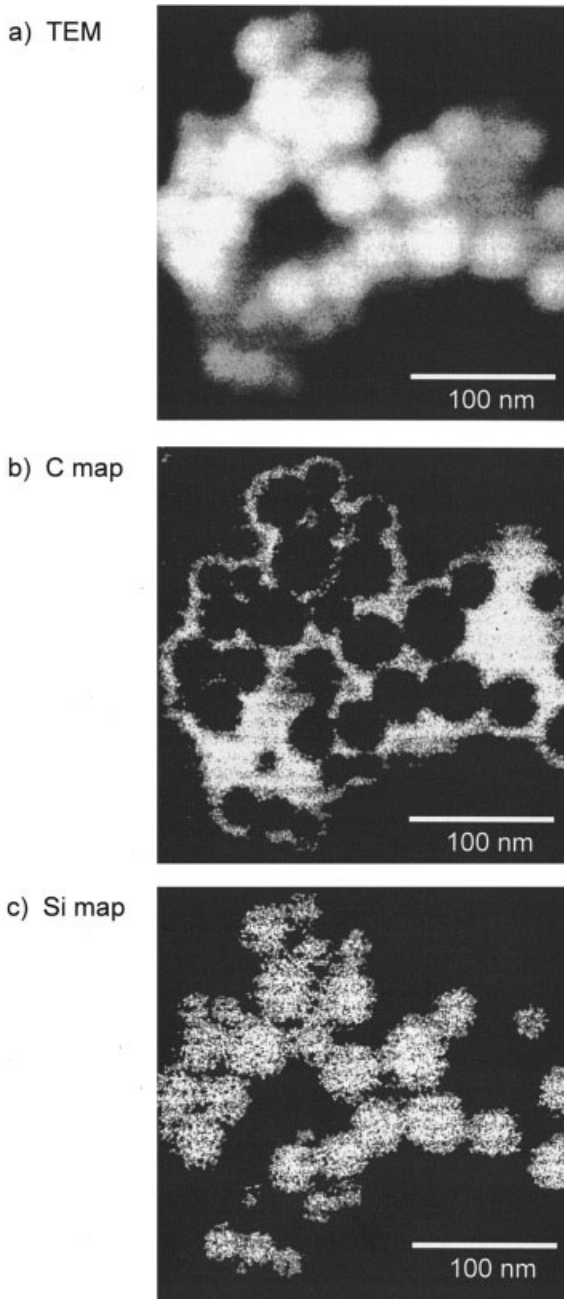

Figure 4 EFTEM images of NCE(46): (a) TEM image of the nano-particles, (b) carbon elemental map revealing the acrylic shells, and (c) silicon elemental map revealing the silica cores.

2(d) shows the DLS chart of the sample prepared in run 5. The comparison of the figure, in which a bimodal distribution at ~ 35 nm and ~ 160 nm is found, with Figure 2(a–c) clearly indicate that the product contained uncovered silica particles in large quantities. Although the larger sized particles may contain core-shell type nanocomposite particles, it is obvious that the effective encapsulation of the silica core can be attained only by the co-usage of nonionic surfactant.

The importance of the surface modification step in the process was also indicated by the runs using NE-30, which has a longer poly(oxyethylene) chain (DP = 30) than NE-10 (DP = 10) on average and has a higher cloud point (>100°C) than NE-10 (40°C) as a result. The emulsion polymerization according to the protocol gave a partly gelling emulsion containing sediments stuck to the inside of a reaction flask and to a stirrer (run 3). The gelation of the emulsion completed on standing the product overnight.

The gelation is considered to be induced by the aggregation of the resulting nanocomposites during the preparation procedure and on standing. This assumption was proved from DLS. The chart of the sample prepared in run 3 [Fig. 3(c)] is bimodal; the peak around 98 nm is due to the primary formed particles and the other is considered to be produced by the aggregation. If the formation of the core-shell type composites is incomplete and the silica core is exposed on the particle surface, the aggregation of the incomplete composites proceeds inevitably as silica sol aggregates by neutralization or drying to form silica gel.

The emulsion polymerization could be performed at 50°C by adopting a redox system. The combination of APS and sodium hydrogen sulfite was effective to complete the polymerization at this temperature. When the whole procedure using NE-10 was carried out at 50°C (run 2), no significant change in the appearance of the system was observed during the surface modification step. Supposedly, NE-10 retains affinity to water at this temperature to some extent as it is a mixture of molecules having distributed length of oligo(oxyethylene) chain, which makes the deposition of NE-10 on the silica surface insufficient. The polymerization gave aggregated emulsion, which caused gelation on standing overnight. The combination of NE-30 with the reaction temperature of 50°C also failed to prepare a homogeneous stable emulsion (run 4). In the absence of SDS, on the other hand, no polymerization of acrylates proceeded in both the pre- and postpolymerization steps. It is of no surprise as NE-10 cannot act as the surfactant at 70°C.

These experimental results indicate the importance of the proper combination on the selection of nonionic surfactant and the polymerization temperature. As the nonionic surfactant lost its surface activity above its cloud point, it is generally used under its cloud point.

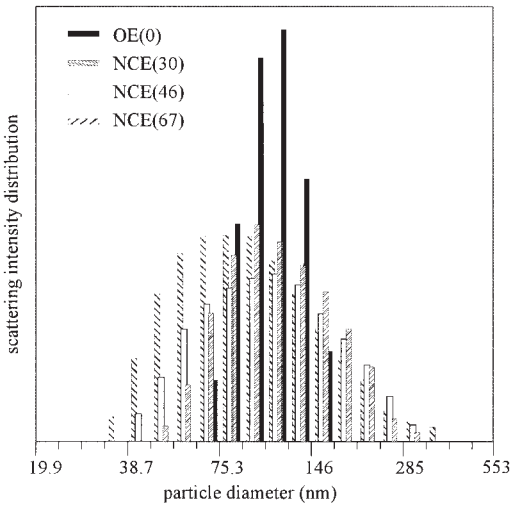

Figure 5 Comparison of particle size distributions of NCEs.

Above the cloud point, hydrogen bonds between the hydrophilic part of the surfactant and water molecules are broken, which causes phase separation. In the present study, we applied this phenomenon to cover the silica particle with the surfactant in the surface modification step, which is considered to be the key feature in our protocol.

With applying this protocol, NCE with different inorganic content could be prepared (runs 1, 7, and 8 in Table I). The inorganic content in the nanocomposites could be increased with no difficulty to 67 wt % by increasing the amount of AT-50. The yield of the nanocomposite, which was measured after drying NCE, was quantitative in any run. The DLS charts of NCEs are compared in Figure 5. The average diameter of the nanocomposite particles tends to decrease according to the increase of the inorganic content as a natural consequence. The distribution of the particle size was broader than that of OE(0) in any run, which was not influenced by the composition.

Preparation of films from NCE

A transparent film was prepared from NCE by casting it on a polyethylene sheet. When NCE was cast on a glass plate, the resulting film could not be peeled off from the plate. Supposedly, the silica part in the hybrid strongly interacted or reacted with the glass surface during the drying process. This high affinity to glass will make NCE an effective surface coating material to glass and other related inorganic materials. A transparent film could also be prepared from a blend of OE(0) and AT-50 (50 : 50 wt/wt). However, it was too brittle to examine its properties. Obviously, the core-shell structure of the nanocomposites improves

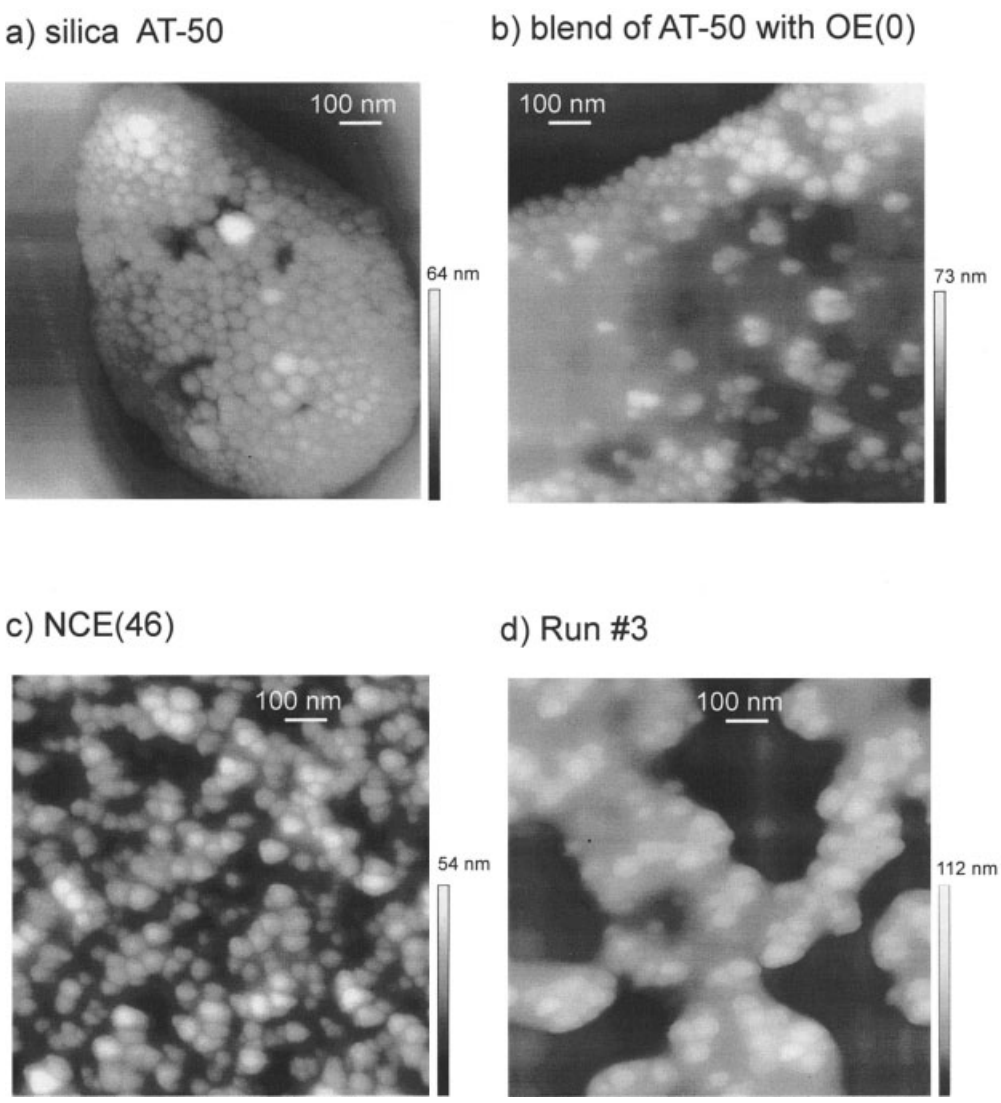

Figure 6 AFM images of the sample emulsions as well as AT-50: (a) silica AT-50, (b) blend of AT-50 with OE(0), (c) NCE(46), and (d) Run #3.

the mechanical properties of the film, which will be described in a succeeding article.

AFM images of the nanocomposites

AFM images measured by the tapping mode are shown in Figure 6. Figure 6(a) is that of AT-50, which was diluted, cast on a mica plate, and dried to prepare the sample. The Figure clearly shows that the silica particles aggregated to form a large secondary particle during the drying process.

Figure 6(b) shows an AFM image of the film prepared from a mixture of AT-50 and OE(0). The silica particles are observed as light gray skewed spheres, and the organic part appears in dim gray. The silica particles gather together and, hence, are unevenly distributed in the film. The sample prepared in run 5 of Table I showed an analogous texture in AFM. Figure 6(c) is an image of a thin film prepared from NCE(46). It is obvious that the silica particles are distributed in the sample film uniformly as they are covered by organic shells.

A significant difference in texture was observed between Figures 6(c,d); the latter is an AFM image of the sample prepared from the emulsion in run 3 in Table I. In the latter image, the silica particles gathered to form secondary particles, which induced phase separation of the inorganic part from the acrylic part in submicron size. This observation proved that the gelation observed during the preparation of this emulsion was induced by the aggregation of the primary formed nanocomposites.

Solubility of the nanocomposite film

We intended to separate the organic part from the silica cores by extracting the film with chloroform to

analyze the composition of the organic part. However, we found that the nanocomposite film gained high resistivity to organic solvents. Solvent resistance has been known as one of the relevant properties when nano-sized silica particles are applied as the filler for polymers.[24,25] The solubility of the nanocomposite film from NCE(46) is compared with the film prepared from OE(0) in Table II. Obviously, the nanocomposite film gained remarkable durability against organic solvents. It was insoluble in ethyl acetate and phenol, and partly soluble in toluene and DMF; each of them was a good solvent for the acrylic film prepared from OE(0). Although we prepared two types of films by changing the drying condition, at room temperature for 2 weeks or at 50°C for 16 h, their solubility was not influenced by the drying condition.

Table III shows the detailed solubility of the composite films to DMF. The solubility decreased according to the decrease of the inorganic content, and the film from NCE(67) was almost insoluble in DMF. These results suggest the strong interaction among the silica particles with keeping interaction with the polymer part. The former will be the SiOSi covalent bonding between the silica particles produced by the loss of water. As T_g of the organic shell (−23°C) is far lower than the drying temperature, the phase separation in nano-scale will proceed during the drying process, which is followed by condensation between the silica cores. As the silica particles distributed in the nanocomposite evenly, the condensation gave an IPN-like structure to the composite, as shown in Figure 6(c), which is considered to increase the resistivity to organic solvents.

Films prepared from nanocomposite emulsions are expected to be an easy way to prepare nanocomposites as the procedure is so simple that we expect that this approach can be applied to a variety of inorganic nano-particles.

CONCLUSIONS

Core-shell type nanocomposite particles consisting of silica (core) and acrylic polymer (shell) were prepared by the simple suspension polymerization of acrylic monomers in the presence of dispersed silica sol. The polymerization consists of four steps: surface modification, prepolymerization, dissolution, and postpolymerization. All steps were found to be indispensable to prepare a stable emulsion of nanocomposite. The other key technique in the present emulsion polymerization is the usage of nonionic surfactant above its cloud point in the surface modification step. The core-shell structure of nanocomposites was confirmed by DLS, TEM, EFTEM, and AFM. Transparent films were prepared by casting these emulsions. Obvious improvement in resistance to organic solvents was found for these films.

TABLE II
Solubility of Nanocomposite Film in Organic Solvents[a]

Sample	Solvents				
	Toluene	Ethyl acetate	DMF	DMSO	Phenol
NCE(46)	±	−	±	+	−
OE(0)	++	++	++	++	++

[a] The sample films (5 × 5 × 0.2 mm, 50mg) were immersed in 6.0g of the solvent and kept at 50°C for 24h.

++, completely soluble; +, mostly soluble; ±, partly soluble; −, insoluble.

TABLE III
Solubility of Nanocomposite Films to DMF[a]

Sample film	Condition for drying	Insoluble portion (wt %)
OE(0)	50°C, 16h	0
OE(0)	23°C, 1 week	0
NCE(30)	50°C, 16h	56
NCE(46)	23°C, 1 week	69
NCE(46)	50°C, 16h	72
NCE(50)	50°C, 16h	89
NCE(67)	50°C, 16h	99

[a]250mg of the polymer film (10 × 10 × 0.25 mm) was immersed in 30g of DMF at 50°C for 24h.

The authors are grateful to Asahi Kasei Corp. for the TEM and EFTEM analyses of the composites and giving us permission to use these figures. This study was partially supported by the Japan Science and Technology Agency.

References

1. Hommel, H.; Touhami, A.; Legrand, A. P. Makromol Chem 1993, 194, 879.
2. Bourgeat-Lami, E. J Nanosci Nanotechnol 2002, 2, 1.
3. Ajayan, P. M.; Schadler, L. S.; Braun, P. V. Nanocomposite Science and Technology; Wiley-VCH: Weinheim, Germany, 2003.
4. Xiong, M.; Wu, L.; Zhou, S.; You, B. Polym Int 2002, 51, 693.
5. Kroker, K.; Schneider, M.; Hamann, K. Prog Org Coatings 1972, 1, 23.
6. Vidal, A.; Donnet, J. B. Bull Chim Soc Fr 1985, 6, 1088.
7. Raiblea, R.; Hamann, K. Adv Colloid Interface Sci 1980, 13, 65.
8. Tsubokawa, N.; Maruyama, K.; Sone, Y.; Shimamura, M. Polym J 1989, 21, 475.
9. Tsubokawa, N.; Kogure, A. J Polym Sci Part A: Polym Chem Ed 1991, 29, 697.
10. Tsubokawa, N. Prog Polym Sci 1992, 17, 417.
11. Yoshinaga, K.; Kondo, A.; Higashitani, K.; Kito, T. Colloids Surf A 1993, 77, 101.
12. Hanson, M.; Eray, B.; Unger, K.; Neimark, A. V.; Schmid, J.; Albert, K.; Bayer, E. Chromatographia 1993, 35, 403.
13. Yoshinaga, K.; Nagao, K. Compos Interface 1994, 2, 95.
14. Yoshinaga, K.; Nagao, K. Polym Adv Technol 1994, 5, 339.
15. Vangani, V.; Rakshit, A. K. K. Angew Makromol Chem 1994, 220, 21.

16. Bauer, F.; Ernst, H.; Decker, U.; Findeisen, M.; Gläsel, H.-J.; Langguth, H.; Hartmann, E.; Mehnert, R.; Peuker, C. Macromol Chem Phys 2000, 201, 2654.
17. Nakamae, K.; Sumiya, K.; Imai, M.; Matsumoto, T. J Adhes Soc Jpn 1980, 16, 4.
18. Luna-Xavier, J.-L.; Bourgeat-Lami, E.; Guyot, A. Colloid Polym Sci 2001, 279, 947.
19. Barther, C.; Hickey, A. J.; Cairns, D. B.; Armes, S. P. Adv Mater 1999, 11, 408.
20. Amalvy, J. I.; Percy, M. J.; Armes, S. P. Langmuir 2001, 17, 4770.
21. Agarwal, G.; Titman, J. J.; Percy, M. J.; Armes, S. P. J Phys Chem B 2003, 107, 12497.
22. Meguro, K.; Yabe, T.; Ishioka, S.; Kato, K.; Esumi, K. Bull Chem Soc Jpn 1986, 59, 3019.
23. Nagai, K.; Ohishi, Y.; Ishiyama, K.; Kuramoto, N. J Appl Polym Sci 1989, 38, 2183.
24. Gläsel, H.-J.; Hartmann, E.; Mehnert, R.; Hirsch, D.; Böttcher, R.; Hormes, J. Nucl Instrum Methods B 1999, 151, 200.
25. Gläsel, H.-J.; Hartmann, E.; Hirsch, D.; Böttcher, R.; Michel, D.; Hormes, J.; Rumpf, H. J Mater Sci 1999, 43, 2319.